

Colossal magnetoresistance effect of the electron-doped manganese oxide $\text{La}_{1-x}\text{Sb}_x\text{MnO}_3$
($x = 0.05, 0.1$)

This article has been downloaded from IOPscience. Please scroll down to see the full text article.

2003 J. Phys.: Condens. Matter 15 4469

(<http://iopscience.iop.org/0953-8984/15/25/314>)

View [the table of contents for this issue](#), or go to the [journal homepage](#) for more

Download details:

IP Address: 171.66.16.121

The article was downloaded on 19/05/2010 at 12:07

Please note that [terms and conditions apply](#).

Colossal magnetoresistance effect of the electron-doped manganese oxide $\text{La}_{1-x}\text{Sb}_x\text{MnO}_3$ ($x = 0.05, 0.1$)

Ping Duan, Guotai Tan, Shouyu Dai, Yueliang Zhou and Zhenghao Chen¹

Laboratory of Optical Physics, Institute of Physics and Centre for Condensed Matter Physics, Chinese Academy of Sciences, PO Box 603, Beijing 100080, People's Republic of China

E-mail: zhchen@aphy.iphy.ac.cn

Received 2 December 2002, in final form 6 May 2003

Published 13 June 2003

Online at stacks.iop.org/JPhysCM/15/4469

Abstract

La–Sb–Mn–O compounds have been prepared by the solid-state reaction of La_2O_3 , Sb_2O_3 and MnCO_3 . The materials have a perovskite structure and exhibit the colossal magnetoresistance (CMR) effect, and the maximum magnetoresistance ratio could reach as high as 60% (at 225 K under 5 T) for $\text{La}_{0.9}\text{Sb}_{0.1}\text{MnO}_3$. The valence states of manganese and antimony have been identified as Mn^{3+} , Mn^{2+} and Sb^{5+} . The temperature dependences of electrical transport and magnetic properties have been studied. The results suggest that the mechanism of CMR for $\text{La}_{1-x}\text{Sb}_x\text{MnO}_3$ is probably due to the double exchange interaction between Mn^{3+} and Mn^{2+} ions.

1. Introduction

The colossal magnetoresistance (CMR) effect in manganite perovskites has drawn worldwide attention recently due to their physical properties and potential application as magnetic sensors. Much of the reported work has focused on the family of manganese perovskite oxides $\text{R}_{1-x}\text{A}_x\text{MnO}_3$, in which R is a trivalent rare earth element, A stands for divalent (alkaline earth) elements such as Ca, Sr, Ba and Pb, and x is the doping level. The charge carriers are holes, i.e. the electrical conductivity type is p-type for this compound. It exhibits the CMR effect and magnetic phase transition at a particular temperature T_C , which is always in company with a metal–insulator transition. These properties were usually explained by the double exchange (DE) interaction between Mn^{3+} and Mn^{4+} ions [1]. As a tetravalent or quivalent cation is substituted for a La site ion of the parent compound LaMnO_3 , the charge carriers of this manganite are electrons and its conducting type is n-type. The study of this electron-doped CMR material is very important, because it might open the door to a new application field and

¹ Author to whom any correspondence should be addressed.

lead to a new function device of whole oxides, which can be used at a wide range of temperatures and operated with low noise and high sensitivity. Studies of electron-doped manganites, including $R_{1-x}Ce_xMnO_3$ in the form of bulk and thin films [2–9] and $La_{1-x}Zr_xMnO_3$ bulk have been reported [10]. According to a previous work, $R_{1-x}Ce_xMnO_3$ showed a metal–insulator transition and ferromagnetism associated with large negative magnetoresistance (MR) similar to $La_{1-x}Ca_xMnO_3$. Ce ions exist in a tetravalent state and the mixed manganese ions were Mn^{2+} and Mn^{3+} in the system. Moreover, Mitra *et al* [8, 9] have already fabricated a p–n diode successfully by combining $La_{1-x}Ce_xMnO_3$ and $La_{1-x}Ca_xMnO_3$ thin films. Recently, we have reported an investigation of a new n-type compound $La_{1-x}Te_xMnO_3$ [11]. Now, we report the study of $La_{1-x}Sb_xMnO_3$ compounds. The reactions of lanthanide oxides and antimony oxides were studied as early as the 1970s [12–14], followed by more reports on the synthetic techniques, crystal structure and properties of $Mn_2Sb_2O_7$ [15–17]. However, no one has investigated the outcomes when Sb_2O_3 , La_2O_3 and $MnCO_3/MnO$ are mixed and reacted. In the following, we discuss the electrical transport and magnetic properties of the new manganese oxide $La_{1-x}Sb_xMnO_3$ ($x = 0.05, 0.1$) fabricated by traditional solid-state reaction. The experiments verified our assumption that $La_{1-x}Sb_xMnO_3$ was an n-type CMR material similar to $La_{1-x}Te_xMnO_3$, $La_{1-x}Ce_xMnO_3$ and $La_{1-x}Zr_xMnO_3$.

2. Synthesis and experimental details

$La_{1-x}Sb_xMnO_3$ ($x = 0.05, 0.1$) compounds were prepared by traditional solid-state reaction. The stoichiometric mixtures of high purity La_2O_3 , Sb_2O_3 and $MnCO_3$ powders were ground, pressed and pre-sintered before it was sintered at 1250 °C for 18 h. The whole heating program occurred in air and the weight of the sample was monitored. During heating, the pellets were laid on Pt bars to avoid the ceramic material below extending to the pellets. The crystal structure of the samples was analysed by means of x-ray diffraction (XRD). Inductively coupled plasma-atomic emission spectroscopy (ICPAES) and energy-dispersive spectroscopy (EDS) quantitative analysis were used to determine the composition [18], with error limits less than 2%. To check the valence state of manganese in the compounds, the temperature dependence of magnetization in the temperature range of 300–1200 K was measured by a magnetic balance system. X-ray photoelectron spectroscopy (XPS) measurement of Sb 3d was carried out, with a resolution of 0.1 eV. The electrical resistivity of the samples was measured by the usual four-point technique in the temperature range 5–300 K in a field up to 5 T. Magnetic measurements were carried out with a superconducting quantum interference device (SQUID) magnetometer.

3. Results and discussion

3.1. Phase and composition analyses

The XRD pattern of $La_{0.9}Sb_{0.1}MnO_3$ is shown in figure 1, in which θ is the Bragg angle. All diffraction peaks are sharp and can be indexed by a hexagonal symmetry as $a = b = 5.5234 \text{ \AA}$ and $c = 6.6782 \text{ \AA}$, $\alpha = \beta = 90^\circ$ and $\gamma = 120^\circ$, and the unit cell volume is about 176.45 \AA^3 . These parameters show that the unit cell is seriously distorted in comparison with a cubic structure, probably because the ionic radii of La^{3+} and Sb^{5+} ions are appreciably different. The ICPAES result shows that the presented $La_{0.9}Sb_{0.1}MnO_3$ sample can be viewed as $La_{0.92}Sb_{0.097}MnO_3$, which almost follows a stoichiometric compound. In addition, EDS quantitative analysis (figure 2) also indicates that the concentrations of La, Sb, and Mn averaged over many grains are very close to the formula $La_{0.9}Sb_{0.1}MnO_3$ for all samples.

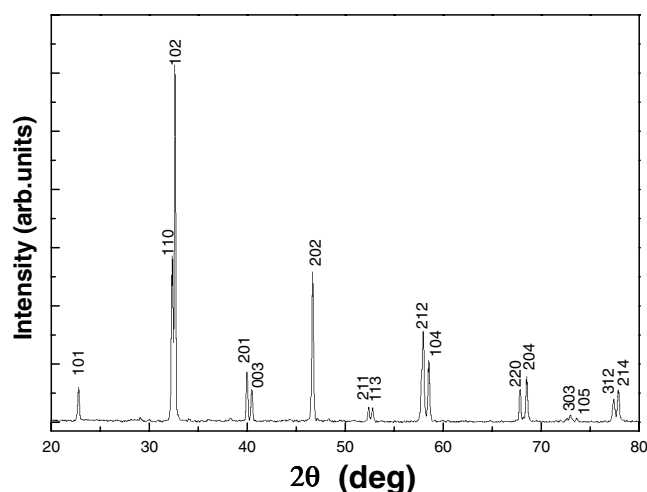


Figure 1. X-ray diffractogram of $\text{La}_{0.9}\text{Sb}_{0.1}\text{MnO}_3$ where θ is the Bragg angle.

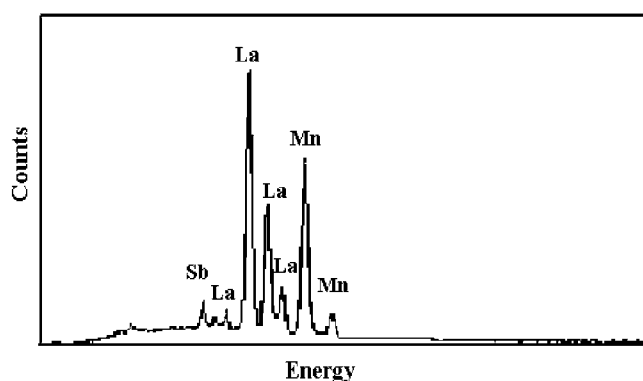


Figure 2. Energy-dispersive spectra (0–24.4 keV) for $\text{La}_{0.9}\text{Sb}_{0.1}\text{MnO}_3$; the percentage of La, Sb, and Mn atoms is 37.49:3.72:38.79 (the ZAF technique)

3.2. Valence states of Mn and Sb

The magnetic-field dependence of magnetization at a temperature of 5 K was measured. The results are presented in figure 3. The magnetization is close to saturation under the field of 5 T and the saturation values for $x = 0.05$ and 0.1 compounds are about 4.1 and 4.6 μ_B per Mn site, respectively. Because the Sb ion was in a +5 valence state, when substituting one Sb for La, two Mn^{3+} ions will be transferred to two Mn^{2+} ions. The experimental values are close to the theoretical values, which suggest that the Mn ions could be in a $\text{Mn}^{3+}/\text{Mn}^{2+}$ mixture valence state, rather than a $\text{Mn}^{3+}/\text{Mn}^{4+}$ mixture in this system.

Furthermore, to identify the valences of manganese in the system, the temperature dependence of magnetization was measured at high temperatures ranging from 300 to 1200 K under a field of 1.2 T, which are shown in figure 4. The samples are in a paramagnetic state in this temperature interval. Although the conductance of the compound follows a polaron conductive law above the Curie temperature, the compounds could be considered as paramagnetic salts, and the magnetic moment of the ions could be described as $g[J(J + 1)]^{1/2}$, where g is the

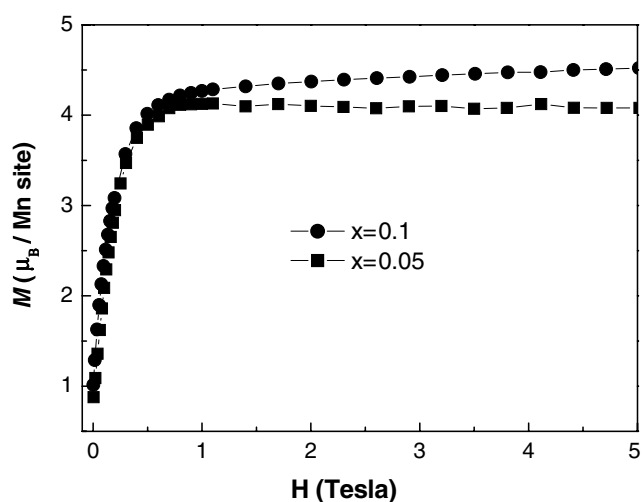


Figure 3. Field dependence of the magnetization at a temperature of 5 K and field range from 0 to 5 T.

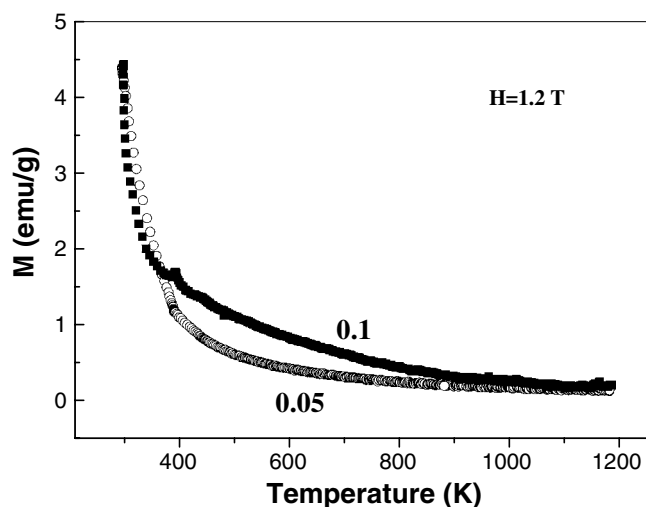


Figure 4. Temperature dependence of the magnetization at high temperatures ranging from 300 to 1200 K.

Landé factor and $J = L + S$ where L is orbital angle momentum and S is spin angle momentum. Based on the electronic configuration of the ions, the magnetic moments of Mn^{2+} , Mn^{3+} and Mn^{4+} are about 5.9 , 4.9 and $3.9 \mu_B$, respectively. They are consistent with the experimental value of manganese salts. The classical theory of Curie's law shows the relation between the Curie constant and the magnetic dipole moment

$$C = N\mu_J^2 / 3k_B\mu_0,$$

$$\mu_{J0.05} / \mu_{J0.1} = (0.9n^{3+} + 0.1n) / (0.8n^{3+} + 0.2n) = (C_{0.05} / C_{0.1})^{1/2},$$

where n^{3+} and n are the number of Bohr magnetons of Mn^{3+} (n_{Bohr}^{3+}) and the other manganese ion, respectively. The Curie constant obtained from the magnetization versus temperature

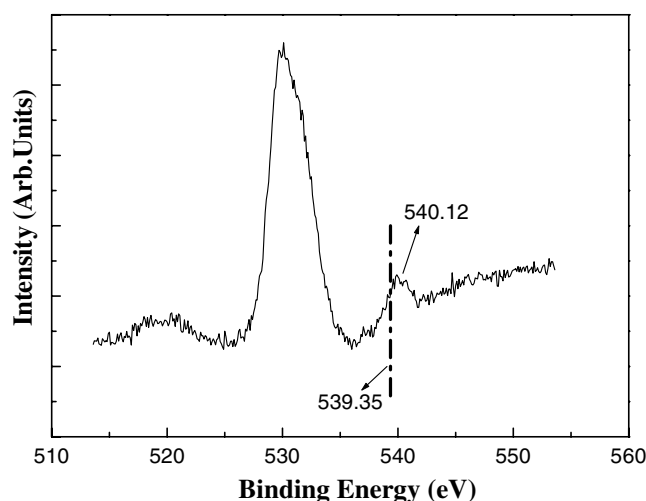


Figure 5. Spectrum of $\text{La}_{0.9}\text{Sb}_{0.1}\text{MnO}_3$. The high peak is the position of O 1s and the other peak is the position of Sb $3d_{3/2}$.

curves is about 0.0098 and 0.01034 for 0.05 and 0.1 samples respectively. If $n^{3+} = 4.9$, then $n \approx 6.2$ was obtained. If we assume the La and O make no contribution to magnetization and the magnetization originates from the Mn ions, $n = 6.2$ is very close to Bohr magneton number of Mn^{2+} (5.9), thus the La–Sb–Mn–O compound could be considered as in a mixing valence state of Mn^{2+} and Mn^{3+} .

In order to identify the valence of antimony, x-ray photoelectron spectroscopy was performed. Only the part of the spectrum near Sb 3d and O 1s is presented here in figure 5. Because $3d_{5/2}$ of antimony is almost at the same position as 1s of oxygen in the spectrum, we have to check $3d_{3/2}$ of antimony to investigate the antimony valence. As shown in figure 5, the high peak is O 1s, while the other peak, located at 540.12 eV, is Sb $3d_{3/2}$. According to the *Handbook of X-ray Photoelectron Spectroscopy* [19], the positions of $3d_{3/2}$ for Sb_2O_3 and Sb_2O_5 should be at 539.35 and 540.15 eV, respectively. The dot–dash line at 539.35 eV in figure 5 indeed shows the deviation from the centre of the small peak, while 540.12 eV is the binding energy of $3d_{3/2}$ for Sb_2O_5 which, within the error range, confirms that the valence of Sb in $\text{La}_{0.9}\text{Sb}_{0.1}\text{MnO}_3$ is +5. Furthermore, the common valences of Sb are +3 and +5; if the valence of Sb is +3 and Sb replaces La(+3), no carriers will occur. So the valence state of antimony is Sb^{5+} and thus $\text{La}_{1-x}\text{Sb}_x\text{MnO}_3$ could be an n-type CMR material.

3.3. Electrical transport and magnetic properties

The temperature dependences of resistivity for the $\text{La}_{0.9}\text{Sb}_{0.1}\text{MnO}_3$ compound under magnetic fields of 0, 1 and 5 T, are shown in figure 6(a). It undergoes a metal–semiconductor (MS) transition at $T_P = 228$ K in zero field; the resistivity exhibits a metallic behaviour ($d\rho/dT > 0$) at low temperature and a semiconductor behaviour ($d\rho/dT < 0$) at high temperature. When a field is applied, $\rho(T)$ is suppressed significantly and T_P shifts a little to a higher temperature (in fields of 0, 1 and 5 T, T_P 227, 229 and 239 K, respectively). The largest change in resistivity takes place around the peak, which gives rise to a prominent negative MR effect. The maximum MR ratio is about 60% in the 5 T field as shown in figure 6(b). The MR ratio, calculated by $\text{MR} = (\rho_0 - \rho_H)/\rho_0$ based on R – T data, also relies strongly on applied magnetic field.

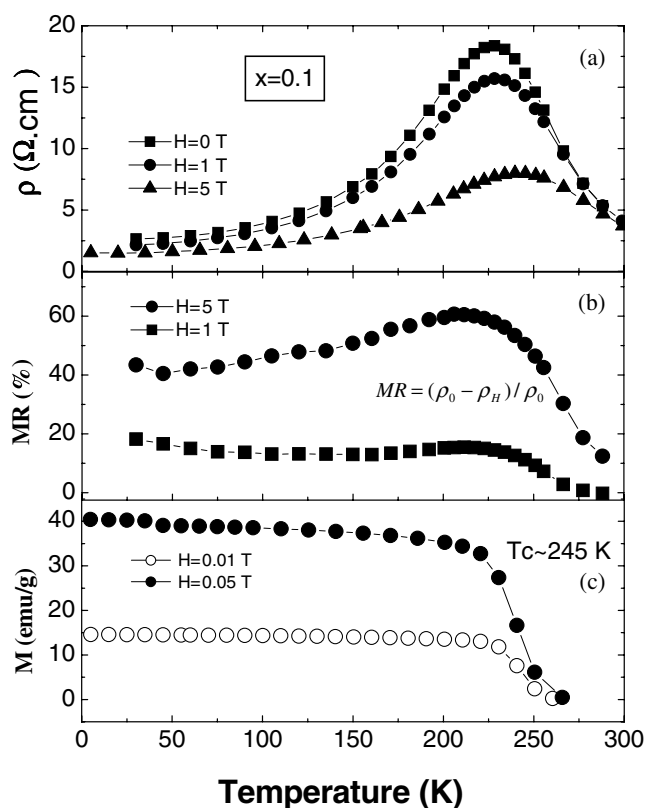


Figure 6. (a) Temperature dependence of the resistivity measured by the standard four-point method. (b) Temperature dependence of the MR ratio. (c) Temperature dependence of the magnetization measured by SQUID.

Figure 6(c) presents the magnetization of the compound as a function of temperature. The magnetization also undergoes a transition from a ferromagnetic state to a paramagnetic state at the Curie temperature ($T_C \approx 245$ K), which is close to T_P , suggesting a correlation between electrical and magnetic transitions.

The temperature dependences of $\rho(T)$, MR and magnetization for the $\text{La}_{0.95}\text{Sb}_{0.05}\text{MnO}_3$ compound are shown in figures 7(a)–(c), respectively. All curves are similar to those of $\text{La}_{0.9}\text{Sb}_{0.1}\text{MnO}_3$. However, the resistivity increases compared with the $\text{La}_{0.9}\text{Sb}_{0.1}\text{MnO}_3$ sample because the carriers decrease when the Sb doping concentration drops. Curie temperatures of both samples were determined, from the peak in the dM/dT versus T curve, to be 245 K ($x = 0.1$) and 240 K ($x = 0.05$). It is worth noting that the $\rho(T)$ and $M(T)$ curves of $\text{La}_{1-x}\text{Ce}_x\text{MnO}_3$ have anomalous (two peaks) behaviour resulting from the impurity phase of MnO_2 [5] or CeO_2 [7], while the $\rho(T)$ and $M(T)$ curves of $\text{La}_{1-x}\text{Sb}_x\text{MnO}_3$ are smooth. This further confirms that the $\text{La}_{1-x}\text{Sb}_x\text{MnO}_3$ ($x = 0.05, 0.1$) compound has a single perovskite phase.

The electrical transport and magnetic properties, and the correlation of both sides for $\text{La}_{1-x}\text{Sb}_x\text{MnO}_3$, are very similar to the hole-doped manganese oxides and could be understood based on the DE model. However, if the DE model is employed in the electron-doped system, it is essential to make some modification, compared with hole-doped system, due to the many

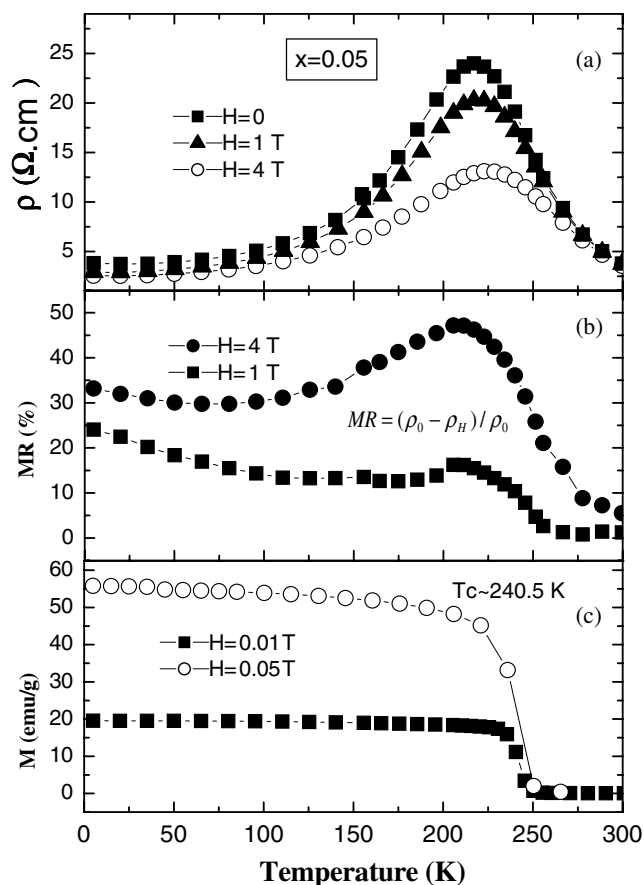


Figure 7. (a) Temperature dependence of the resistivity measured by the standard four-point method. (b) Temperature dependence of the MR ratio. (c) Temperature dependence of the magnetization measured by SQUID magnetometer.

differences between the systems, such as electronic configurations being $(t_{2g}^3 e_g^2)$, $(t_{2g}^3 e_g^1)$ and (t_{2g}^3) for Mn^{2+} , Mn^{3+} and Mn^{4+} , respectively. Also, the sums of the spin are $S = 5/2$, 2 and $3/2$ for Mn^{2+} , Mn^{3+} and Mn^{4+} , respectively, and, according to [20], the 3d state densities of Mn^{4+} and Mn^{2+} are different from each other, calculated by the LSDA method. All of these lead to the difference between the wavefunction Ψ and Hamiltonian H in calculating the function of DE model. Because the intrinsic properties of the compounds are certainly influenced by other factors such as crystal structure etc, it is necessary to further study the effect of these factors on the properties and fabricating technology of the $\text{La}_{1-x}\text{Sb}_x\text{MnO}_3$ films. Detailed theory work is required.

4. Conclusion

In summary, single perovskite phase $\text{La}_{1-x}\text{Sb}_x\text{MnO}_3$ ($x = 0.05, 0.1$) compounds have been fabricated by traditional solid-state reaction for the first time. Analyses have indicated that the valence states of Mn and Sb are Mn^{3+} , Mn^{2+} and Sb^{5+} in this system. Electrical transport and magnetic properties indicate that the compounds are typical CMR materials with about

60% MR in a field of 5 T. The resistivity transition temperature T_P is about 228 K for the $\text{La}_{0.9}\text{Sb}_{0.1}\text{MnO}_3$ sample.

Acknowledgments

We thank Shiyong Fan at Institute of Physics, CAS for allowing us the use of SQUID magnetometer and Fen Liu at Institute of Chemistry, CAS for performing XPS analysis.

References

- [1] Zener C 1951 *Phys. Rev.* **82** 403
De Gennes P-G 1960 *Phys. Rev.* **118** 141
- [2] Maignan A, Martin C and Raveau B 1997 *Z. Phys. B* **102** 19
- [3] Das S and Mandal P 1997 *Z. Phys. B* **104** 7
- [4] Mandal P and Das S 1997 *Phys. Rev. B* **56** 15073
- [5] Gebhardt J R, Roy S and Ali N 1999 *J. Appl. Phys.* **85** 5390
- [6] Raychaudhuri P, Mukherjee S, Nigam A K, John J, Vaisnav U D, Pinto R and Mandal P 1999 *J. Appl. Phys.* **86** 5718
- [7] Mitra C, Raychaudhuri P, John J, Dhar S K, Nigam A K and Pinto R 2001 *J. Appl. Phys.* **89** 524
- [8] Mitra C, Raychaudhuri P, Kobernik G, Dorr K, Muller K-H, Schultz L and Pinto R 2001 *Appl. Phys. Lett.* **79** 2408
- [9] Mitra C, Kobernik G, Dorr K, Muller K-H, Schultz L, Raychaudhuri P, Pinto R and Wieser E 2002 *J. Appl. Phys.* **91** 7715
- [10] Roy S and Ali N 2001 *J. Appl. Phys.* **89** 7425
- [11] Tan G T, Dai S Y, Duan P, Zhou Y L, Lu H B and Chen Z H 2003 *J. Appl. Phys.* **93** 1
- [12] Adachi G, Kawahito T, Matsumoto H and Shiokawa J 1970 *J. Inorg. Nucl. Chem.* **32** 686
- [13] Nath D K 1970 *Inorg. Chem.* **9** 2714
- [14] Adachi G, Ishihara M and Shiokawa J 1973 *J. Less-Common Met.* **32** 175
- [15] Brisse F, Stewart D J, Seidl V and Knop O 1972 *J. Chem.* **50** 3648
- [16] Subramanian M A, Clearfield A, Umarji A M, Shenoy G K and Subba Rao G V 1984 *J. Solid State Chem.* **52** 124
- [17] Scott H G 1987 *J. Solid State Chem.* **66** 171
- [18] Li Z W, Morrish A H and Jiang J Z 1999 *Phys. Rev. B* **60** 10284
- [19] Wagner C D, Riggs W M, Davis L E, Moulder J F and Muilenberg G E 1979 *Handbook of X-ray Photoelectron Spectroscopy* (Eden Prairie, MN: Perkin-Elmer Corporation Physical Electronics Division) p 6509
- [20] Kang J-S, Kim Y J, Lee B W, Olson C G and Min B I 2001 *J. Phys.: Condens. Matter* **13** 3779